Optimization of magnetoelectricity in piezoelectric–magnetostrictive bilayers

2010 Smart Mater. Struct. 19 125010

(http://iopscience.iop.org/0964-1726/19/12/125010)

Smart Mater. Struct. **19** (2010) 125010 (13pp) doi:10.1088/0964-1726/19/12/125010

Optimization of magnetoelectricity in piezoelectric–magnetostrictive bilayers

Hsin-Yi Kuo[1], **Alex Slinger**[2] **and Kaushik Bhattacharya**[3]

[1] Department of Civil Engineering, National Chiao Tung University, Hsinchu 30010, Taiwan
[2] Department of Engineering, University of Cambridge, Cambridge CB2 1PZ, UK
[3] Division of Engineering and Applied Science, California Institute of Technology, Pasadena, CA 91125, USA

E-mail: bhatta@caltech.edu

Received 10 May 2010, in final form 25 August 2010
Published 1 November 2010
Online at stacks.iop.org/SMS/19/125010

Abstract
Magnetoelectric coupling is of interest for a variety of applications, but is weak in monolithic materials. Strain-coupled bilayers or multilayers of piezoelectric and magnetostrictive material are an attractive way of obtaining enhanced effective magnetoelectricity. This paper studies the optimization of magnetoelectricity with respect to the crystallographic orientations and the relative thickness of the two materials. We show that the effective transverse ($\alpha_{E,31}$) and longitudinal ($\alpha_{E,33}$) coupling constants can be enhanced many-fold at the optimal orientation compared to those at normal orientation. For example, we show that the constants are 17 and 7 times larger for the optimal orientation of a lithium niobate/Terfenol-D bilayer of equal thickness compared to the normal orientation. The coupling also increases as the piezoelectric phase gets thinner.

(Some figures in this article are in colour only in the electronic version)

1. Introduction

Magnetoelectricity (ME) refers to the magnetization induced by an electric field, or conversely the polarization induced by a magnetic field. The study of magnetoelectricity can be traced back to 1957 when Landau and Lifshitz [1] showed the possibility of the existence of a linear relationship between the electric and magnetic fields in a substance with a certain magnetic symmetry class. This was subsequently experimentally confirmed in an antiferromagnetic single-crystal Cr_2O_3 by Astrov [2] who measured the magnetization response to an electric field, and by Rado and Folen [3] who detected the polarization induced by a magnetic field.

This ME effect is of interest to important technological applications. It can provide large-area and sensitive detection of magnetic fields. It can be the basis of a four-state memory element. It can also be the basis of exotic optical devices. However, this coupling is limited to monolithic or single-phase materials, and is often observed only at very low temperatures. For instance, Cr_2O_3 has the magnetoelectric voltage coefficient of 0.02 V cm^{-1} Oe^{-1} [4] below the antiferromagnetic Néel temperature of 307 K [5]. This is insufficient for practical applications.

To overcome this limitation of natural materials, various researchers have turned to composite media, as explained in recent reviews by Eerenstien *et al* [6] and Nan *et al* [7]. The basic idea is to couple a magnetostrictive and a piezoelectric material using strain: an applied magnetic field creates a strain in the magnetostrictive material which in turn creates a strain in the piezoelectric material, resulting in an electric polarization. Bilayers or laminates are particularly attractive since the strain coupling is extremely strong. Indeed, the highest ME coefficients amongst all known materials and composites have been reported in bilayers [6–9].

The promise of applications, and the indirect coupling through strain has also made magnetoelectric composites the topic of a number of theoretical investigations. Harshe *et al* [10] and Avellaneda and Harshe [11], in their pioneering works on magnetoelectric composites, proposed a theoretical model for a multilayer (2-2) structure. They computed the longitudinal ME voltage coefficient assuming ideal coupling at the interface and longitudinal orientation of the poling and magnetic axes. They also obtained the optimal volume fraction for energy transfer. Nan [12] proposed a general theoretical framework based on a Green's function method and perturbation theory and provided exact

and approximate results for the magnetoelectric coefficient in various special geometries. Benveniste [13] developed a theory for magnetoelectric coupling in fibrous composites assuming that the poling and magnetic directions are parallel to the fibers. Li and Dunn [14] developed a Mori–Tanaka-based micromechanics approach to analyze the average fields and effective moduli of the ME composite, and gave explicit expressions for the effective moduli of fibrous and laminated composites. In recent years, multilayer composites have been the subject of numerous investigations. Notable among them is the averaging method of Bichurin *et al* [15–17] that has been applied to perfectly bonded and unclamped bilayers [15, 16] as well as imperfectly bonded and clamped bilayers [17]. A complete review of all this literature can be found in Nan *et al* [7] and Bichurin [18]. Importantly, much of this theoretical development limits itself to the situation where the poling direction of the piezoelectric material and the magnetic axes of the piezomagnet/magnetostrictive material is either normal to or along the layer (or fiber) direction. Further, many of these works assume transverse isotropy or uniaxial symmetry.

Single crystals, or bilayers made of single-crystal layers, promise further and significant enhancement of the magnetoelectric coupling. However, single crystals are highly anisotropic and it is not clear how they should be oriented with respect to the layer normal for optimal ME coupling. Recent advances in wafer bonding and layer transfer enables the fabrication of high quality single-crystal ferroelectric films of potentially arbitrary orientations on diverse substrates [19]. Indeed, experiments by Yang *et al* [20] and Wang *et al* [21] show that single crystals are attractive and the effective ME coefficient of the laminate can depend sensitively on the crystallographic orientation of the material.

Motivated by these advances, and in a departure from previous works, we develop a method to calculate the effective ME coefficient of a bilayer without any assumptions on the symmetry of the underlying materials and without any assumptions on the crystallographic orientations of the materials. We then optimize the crystallographic orientation and volume fraction, and demonstrate our method and its efficacy using lithium niobate/Terfenol-D as well as lithium niobate/$CoFe_2O_4$ bilayers. We show that the optimal orientations can be non-trivial and the enhancement to be manifold over the normal orientations.

2. Model

Consider a bilayer or laminate of piezoelectric and magnetostrictive material as shown in figure 1. We assume that the thickness is much smaller than the lateral extent or in-plane dimensions. Since the layers are strain-coupled, the bilayer shown on the left will suffer from some bending while the more symmetric laminate shown on the right will not. However, the strains associated with bending will be smaller compared to those associated with lateral extension. Further, they will be vanishingly small if the thickness of one layer is small compared to the other. Therefore we do not make a distinction between the two geometries.

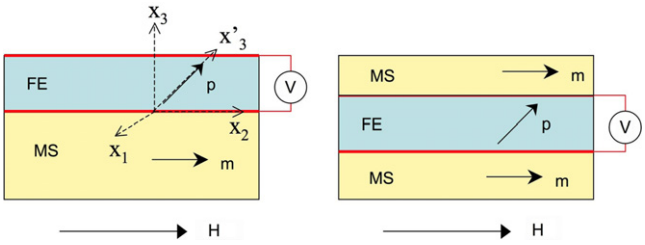

Figure 1. The bilayer and laminate configurations.

2.1. Constitutive relations

In a Cartesian frame with the x_3 direction normal to the plane, the constitutive relations of the piezoelectric material (superscript p) are

$$\varepsilon_{ij}^{\mathrm{p}} = s_{ijkl}^{\mathrm{p,E}}\sigma_{kl}^{\mathrm{p}} + d_{kij}E_k, \tag{1}$$

$$D_i = d_{ijk}\sigma_{jk}^{\mathrm{p}} + \epsilon_{ij}^{\sigma}E_j, \tag{2}$$

where $\varepsilon_{ij}^{\mathrm{p}}$ and σ_{ij}^{p} are the strain and stress; E_i and D_i are the electric field and the electric displacement vector. $s_{ijkl}^{\mathrm{p,E}}$ is the (constant field) elastic compliance (fourth-order tensor), d_{ijk} is the piezoelectric moduli (third-order) and ϵ_{ij}^{σ} is the (constant stress) permittivity (second-order). We assume that the piezoelectric material is magnetically inert. The summation convention is used. The constitutive law of magnetostrictive material (superscript m) is

$$\varepsilon_{ij}^{\mathrm{m}} = s_{ijkl}^{\mathrm{m},H}\sigma_{kl}^{\mathrm{m}} + \lambda_{ij}(H_k), \tag{3}$$

where H_i is the applied magnetic field, $s_{ijkl}^{\mathrm{m},H}$ is the (constant field) compliance and λ_{ij} is the magnetostriction that depends nonlinearly on the magnetic field. We have not written the equation for the magnetic moment since we do not need it in our calculations. The nonlinear magnetoelectric response is often undesirable in applications, and therefore it is used in a linear piezomagnetic regime with a small applied field (and possibly a constant bias field). We then linearize λ_{ij} and write it as $\lambda_{ij} = q_{kij}H_k$, where q_{ijk} is the piezomagnetic moduli (third-order tensor).

The equations above refer the material properties (ϵ_{ij}, d_{ijk}, s_{ijkl}, λ_{ij}, q_{ijk}) to the laminate frame (figure 1). However, the material properties are commonly described in the crystallographic frame and we need to transform them to the laminate frame. To this end, let us denote the crystal frame with primes and introduce the rotation matrix a_{ij}. This is given in terms of the three Euler angles (α, β, γ) as follows [22]:

$$\begin{pmatrix} a_{11} & a_{12} & a_{13} \\ a_{21} & a_{22} & a_{23} \\ a_{31} & a_{32} & a_{33} \end{pmatrix} = \begin{pmatrix} \cos\gamma\cos\alpha - \cos\beta\sin\alpha\sin\gamma & \cos\gamma\sin\alpha + \cos\beta\cos\alpha\sin\gamma & \sin\gamma\sin\beta \\ -\sin\gamma\cos\alpha - \cos\beta\sin\alpha\cos\gamma & -\sin\gamma\cos\alpha + \cos\beta\cos\alpha\cos\gamma & \cos\gamma\sin\beta \\ \sin\beta\sin\alpha & -\sin\beta\cos\alpha & \cos\beta \end{pmatrix}. \tag{4}$$

For this change of frame, the material parameters then follow the tensor transformation rules for second- , third- and fourth-

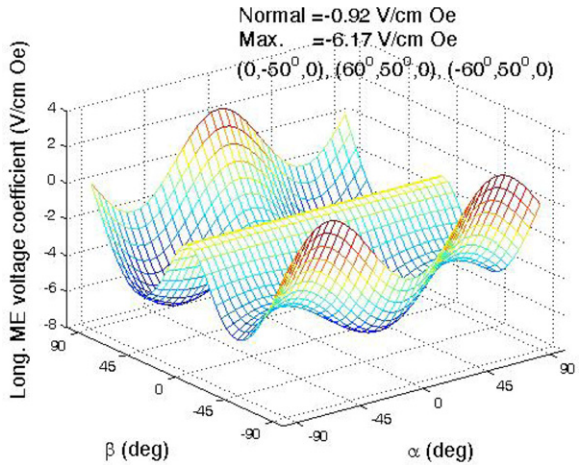

Figure 2. The longitudinal ME voltage coefficient of a $LiNbO_3$/Terfenol-D bilayer for various orientations of $LiNbO_3$. Note that this coefficient depends only on the Euler angles α and β and is independent of the third, γ.

order tensors:

$$\epsilon_{ij} = a_{im}a_{jn}\epsilon'_{mn}, \qquad \lambda_{ij} = a_{im}a_{jn}\lambda'_{mn},$$
$$d_{ijk} = a_{im}a_{jn}a_{ko}d'_{mno}, \qquad q_{ijk} = a_{im}a_{jn}a_{ko}q'_{mno}, \tag{5}$$
$$s_{ijkl} = a_{im}a_{jn}a_{ko}a_{lp}s'_{mnop}.$$

where the primed quantities ($\epsilon'_{ij}, d'_{ijk}, s'_{ijkl}, \lambda'_{ij}, q'_{ijk}$) denote the material properties referred to the crystallographic frame.

2.2. Field equations, boundary conditions and interface conditions

In the bilayer and laminate geometry, the fields, displacement current and strains are constant in each layer up to leading order. Thus the field equations are automatically satisfied.

We assume that there are no applied external stresses. Therefore the tractions on the top and bottom surfaces as well as the average tractions on the lateral surfaces are constant. This implies

$$\sigma^{\mathrm{p,m}}_{i3} = 0, \qquad i = 1, 2, 3, \tag{6}$$

$$\sigma^{\mathrm{p}}_{ij}v^{\mathrm{p}} + \sigma^{\mathrm{m}}_{ij}v^{\mathrm{m}} = 0, \qquad i, j = 1, 2, \tag{7}$$

where $v^{\mathrm{p,m}}$ are the volume fractions. We assume that the interfaces are perfectly bonded so that the tangential strains are continuous [23]:

$$\varepsilon^{\mathrm{p}}_{ij} = \varepsilon^{\mathrm{m}}_{ij}, \qquad i, j = 1, 2. \tag{8}$$

We note that (6) automatically ensures traction continuity at the interface.

We assume that the interface is perfectly electromechanically bonded so that the tangential electric and magnetic fields are continuous, the jump in normal displacement current is equal to the surface charge (with density σ) and the normal magnetic induction is continuous [24]:

$$E^{\mathrm{p}}_1 = E^{\mathrm{m}}_1, \qquad E^{\mathrm{p}}_2 = E^{\mathrm{m}}_2, \qquad D^{\mathrm{p}}_3 - D^{\mathrm{m}}_3 = 4\pi\sigma, \tag{9}$$

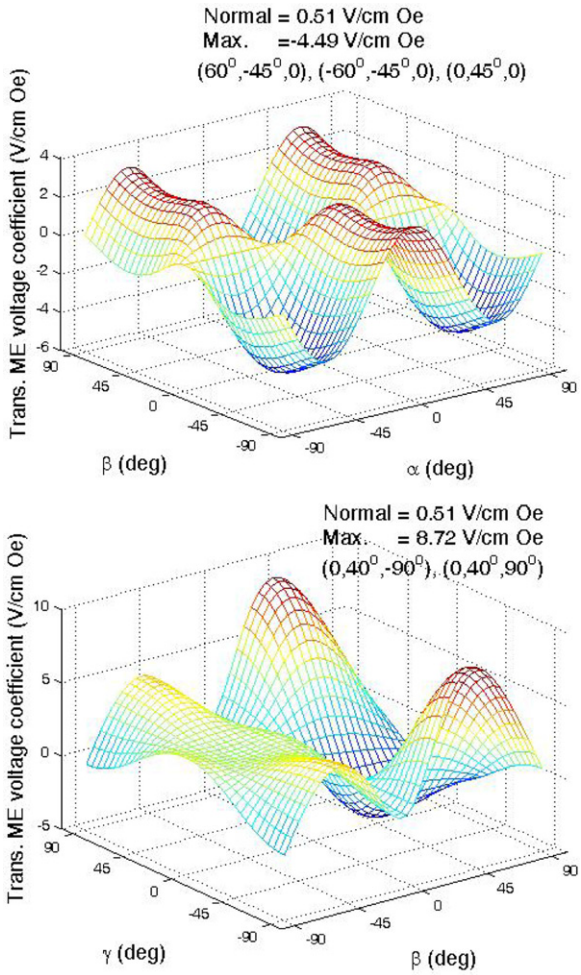

Figure 3. The transverse ME voltage coefficient of a $LiNbO_3$/Terfenol-D bilayer for various orientations of $LiNbO_3$.

$$H^{\mathrm{p}}_1 = H^{\mathrm{m}}_1, \qquad H^{\mathrm{p}}_2 = H^{\mathrm{m}}_2, \qquad B^{\mathrm{p}}_3 = B^{\mathrm{m}}_3. \tag{10}$$

There are two situations when it comes to the electrical conditions since metallic magnetic materials are electrically conducting while ceramic magnets are not. Therefore we distinguish between two situations.

2.2.1. Electrically conducting magnetic layer. Here, the in-plane electric field is zero and the top/bottom surfaces are equipotential in the magnetic material, and thus we have

$$E^{\mathrm{m}}_1 = E^{\mathrm{m}}_2 = D^{\mathrm{m}}_3 = 0. \tag{11}$$

We are interested in finding the electric field in the piezoelectric material, and thus consider an open circuit situation. Therefore $\sigma = 0$. From the interfacial condition (9), we conclude

$$E^{\mathrm{p}}_1 = E^{\mathrm{p}}_2 = D^{\mathrm{p}}_3 = 0. \tag{12}$$

2.2.2. Electrically insulating magnetic layer. Here the displacement current is zero in the magnetic layer and we thus have

$$D^{\mathrm{m}}_1 = D^{\mathrm{m}}_2 = D^{\mathrm{m}}_3 = 0. \tag{13}$$

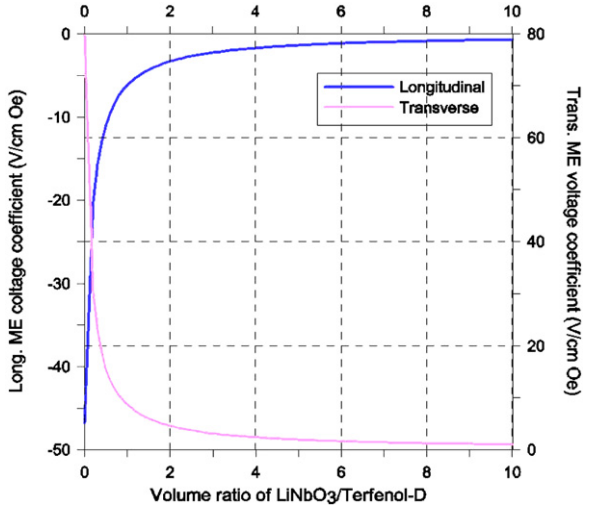

Figure 4. The optimal ME voltage coefficients of a $LiNbO_3$/Terfenol-D bilayer for various volume ratios of $LiNbO_3$/Terfenol-D.

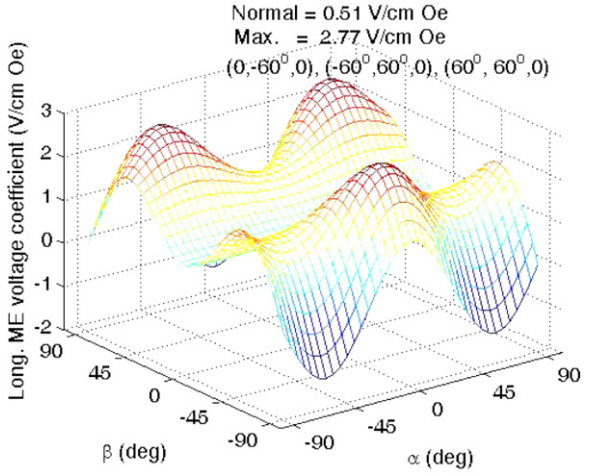

Figure 5. The longitudinal ME voltage coefficient of a $LiNbO_3/CoFe_2O_4$ bilayer for various orientations of $LiNbO_3$. Note that this coefficient depends only on the Euler angles α, β and is independent of the third γ.

Again, we consider open circuit conditions together with the in-plane open circuit in the piezoelectric layer so that we conclude from (10) that

$$D_1^{\mathrm{p}} = D_2^{\mathrm{p}} = D_3^{\mathrm{p}} = 0. \tag{14}$$

2.3. Effective magnetoelectric response

We seek to compute the effective magnetoelectric response. For the linear case of piezomagnetic material, the induced voltage is proportional to the applied magnetic field and the constant of proportionality is the effective magnetoelectric voltage coefficient.

We begin by computing the magnetoelectric voltage coefficients for the case of the electrically conducting magnetic layer. We switch from the tensorial notation above to the Voigt notation. We are given $\mathbf{H} = \{H_1, 0, H_3\}$ and seek to

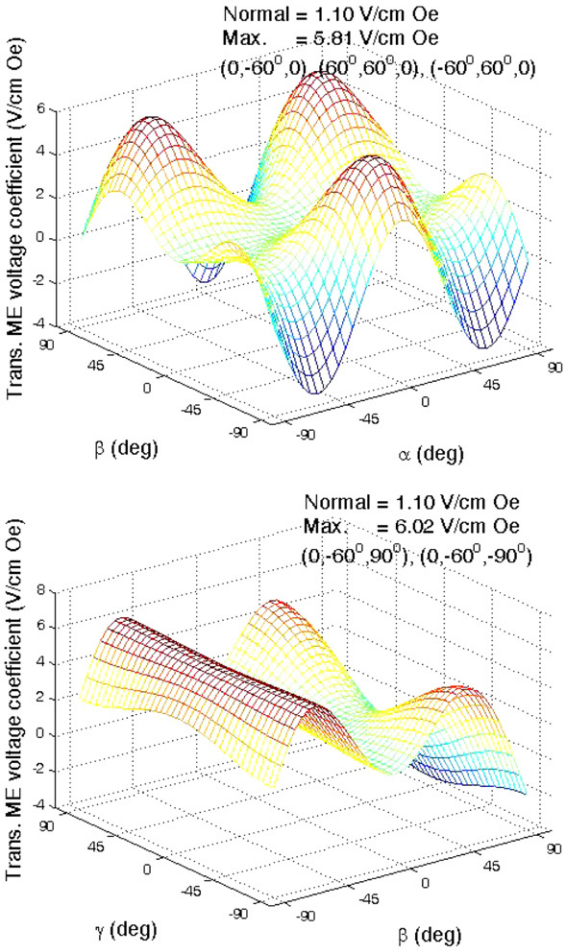

Figure 6. The transverse ME voltage coefficient of a $LiNbO_3/CoFe_2O_4$ bilayer for various orientations of $LiNbO_3$.

find $\mathbf{E}^{\mathrm{p}}$. In light of equation (6), the only unknown stresses are σ_1, σ_2 and σ_6. Further, in light of equation (7), we can obtain the stress components σ_i^{m} in the magnetic layer from those in the piezoelectric layer σ_i^{p}. Thus, the only unknown stresses are $\sigma_1^{\mathrm{p}}, \sigma_2^{\mathrm{p}}$ and σ_6^{p}. Similarly, in light of equation (12), the electrical unknowns are D_1^{p}, D_2^{p} and E_3^{p}. To solve for these unknowns, we substitute equations (1) and (3) into equation (8) and rewrite equation (2) using equation (12). These equations, (8) and (2), may now be written compactly as follows in terms of the unknown quantities:

$$\begin{bmatrix} s_{11}^{\mathrm{p}} + f s_{11}^{\mathrm{m}} & s_{12}^{\mathrm{p}} + f s_{12}^{\mathrm{m}} & s_{16}^{\mathrm{p}} + f s_{16}^{\mathrm{m}} & 0 & 0 & d_{31} \\ s_{21}^{\mathrm{p}} + f s_{21}^{\mathrm{m}} & s_{22}^{\mathrm{p}} + f s_{22}^{\mathrm{m}} & s_{26}^{\mathrm{p}} + f s_{26}^{\mathrm{m}} & 0 & 0 & d_{32} \\ s_{61}^{\mathrm{p}} + f s_{61}^{\mathrm{m}} & s_{62}^{\mathrm{p}} + f s_{62}^{\mathrm{m}} & s_{66}^{\mathrm{p}} + f s_{66}^{\mathrm{m}} & 0 & 0 & d_{36} \\ d_{11} & d_{12} & d_{16} & -1 & 0 & \epsilon_{13} \\ d_{21} & d_{22} & d_{26} & 0 & -1 & \epsilon_{23} \\ d_{31} & d_{32} & d_{36} & 0 & 0 & \epsilon_{33} \end{bmatrix} \times \begin{bmatrix} \sigma_1^{\mathrm{p}} \\ \sigma_2^{\mathrm{p}} \\ \sigma_6^{\mathrm{p}} \\ D_1^{\mathrm{p}} \\ D_2^{\mathrm{p}} \\ E_3^{\mathrm{p}} \end{bmatrix} = \begin{bmatrix} q_{11}H_1 + q_{31}H_3 \\ q_{12}H_1 + q_{32}H_3 \\ q_{16}H_1 + q_{36}H_3 \\ 0 \\ 0 \\ 0 \end{bmatrix} \tag{15}$$

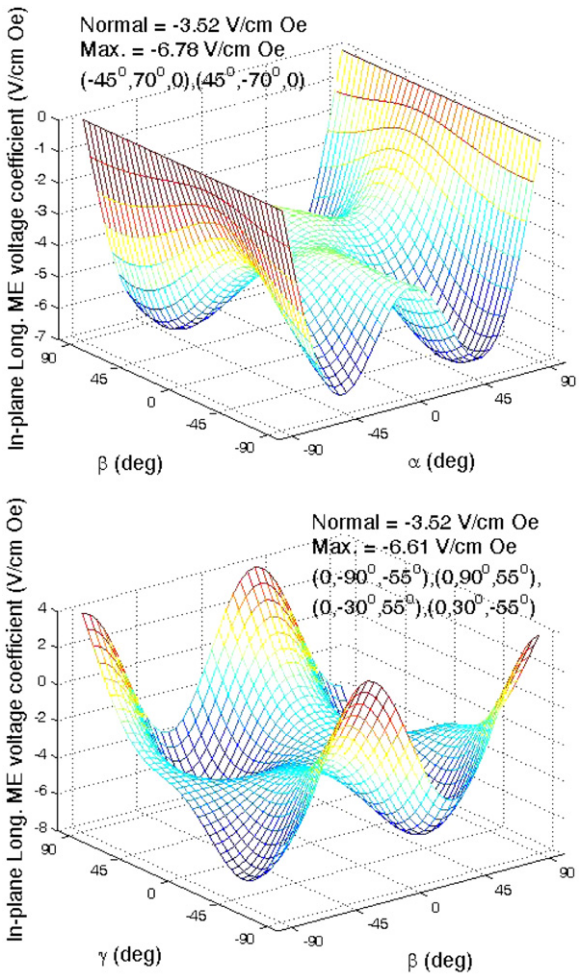

Figure 7. The in-plane longitudinal ME voltage coefficient of a $LiNbO_3/CoFe_2O_4$ bilayer for various orientations of $LiNbO_3$.

where f is the volume ratio, $v^{\mathrm{p}}/v^{\mathrm{m}}$, between the piezoelectric and piezomagnetic materials.

We can verify that the matrix of material coefficients on the left is not singular, and hence we can invert it to find the unknown stresses, electric displacements and electric field. Clearly, the transverse electric field E_3^{p} depends linearly on the applied magnetic field. Setting $H_1 = 0$, we can obtain the *longitudinal magnetoelectric voltage coefficient* $\alpha_{E,33} = E_3^{\mathrm{p}}/H_3$ which describes the out-of-plane electric field due to the applied out-of-plane magnetic field. Similarly, setting $H_3 = 0$, we can obtain the *transverse magnetoelectric voltage coefficient* $\alpha_{E,31} = E_3^{\mathrm{p}}/H_1$ which describes the out-of-plane electric field due to the applied in-plane magnetic field.

The matrix in equation (15) is too complicated to invert in closed form for a general anisotropy and general orientation. So we proceed numerically in the general case and present detailed results in section 3. For now, we note that, in the special case of an uniaxial piezoelectric with normal orientation, many of the coefficients are zero and we can obtain the coefficients in closed form:

$$\alpha_{E,33} = \frac{E_3^{\mathrm{p}}}{H_3} = \frac{-2d_{31}q_{31}}{\epsilon_{33}\left(s_{11}^{\mathrm{p}} + s_{12}^{\mathrm{p}}\right) + f\epsilon_{33}\left(s_{11}^{\mathrm{m}} + s_{12}^{\mathrm{m}}\right) - 2d_{31}^2}, \tag{16}$$

Table 1. Material constants of $LiNbO_3$ [27], PZT [28], Terfenol-D [29, 30] and $CoFe_2O_4$ [14, 31]. (Note: units: **s**: 10^{-12} m^2 N^{-1}, **d**: 10^{-11} C N^{-1}, **q**: 10^{-7} Oe^{-1}, $\epsilon_0 = 8.854 \times 10^{-12}$ F m^{-1}. Constants assume materials polarized/magnetized along the x_3 axis.)

Property	$LiNbO_3$ ($3m$)	PZT-5A ($6mm$)	Property	Terfenol-D ($6mm$)	$CoFe_2O_4$ ($6mm$)
$s_{11}^{\mathrm{p,E}}$	5.55	16.4	$s_{11}^{\mathrm{m},H}$	38.4	6.47
$s_{12}^{\mathrm{p,E}}$	−1.04	−5.74	$s_{12}^{\mathrm{m},H}$	−10.6	−2.38
$s_{13}^{\mathrm{p,E}}$	−1.3	−7.22	$s_{13}^{\mathrm{m},H}$	−13.6	−2.58
$s_{14}^{\mathrm{p,E}}$	−0.98	0	$s_{33}^{\mathrm{m},H}$	45.4	6.97
$s_{33}^{\mathrm{p,E}}$	4.8	18.8	$s_{44}^{\mathrm{m},H}$	73.5	22.08
$s_{44}^{\mathrm{p,E}}$	20.6	47.5	$s_{66}^{\mathrm{m},H}$	63.7	17.70
d_{15}	7.7	58.4	q_{15}	6.34	9.66
d_{22}	1.7	0	q_{31}	−3.05	0.45
d_{31}	−0.13	−17.1	q_{33}	6.99	1.50
d_{33}	0.66	37.4			
$\epsilon_{11}^{\sigma}/\epsilon_0$	84	1730	$\lambda_{\parallel}$	2×10^{-3}	-6×10^{-5}
$\epsilon_{33}^{\sigma}/\epsilon_0$	30	1700	$\lambda_{\perp}$	-2.26×10^{-3}	7×10^{-5}

$$\alpha_{E,31} = \frac{E_3^{\mathrm{p}}}{H_1} = \frac{-d_{31}(q_{11} + q_{12})}{\epsilon_{33}\left(s_{11}^{\mathrm{p}} + s_{12}^{\mathrm{p}}\right) + f\epsilon_{33}\left(s_{11}^{\mathrm{m}} + s_{12}^{\mathrm{m}}\right) - 2d_{31}^2}. \tag{17}$$

These are in agreement with those reported in the literature [25].

We follow a very similar procedure in the electrically insulating magnetic layer, replacing equation (12) with equation (14). We obtain the following system of equations:

$$\begin{bmatrix} s_{11}^{\mathrm{p}} + fs_{11}^{\mathrm{m}} & s_{12}^{\mathrm{p}} + fs_{12}^{\mathrm{m}} & s_{16}^{\mathrm{p}} + fs_{16}^{\mathrm{m}} & d_{11} & d_{21} & d_{31} \\ s_{21}^{\mathrm{p}} + fs_{21}^{\mathrm{m}} & s_{22}^{\mathrm{p}} + fs_{22}^{\mathrm{m}} & s_{26}^{\mathrm{p}} + fs_{26}^{\mathrm{m}} & d_{12} & d_{22} & d_{32} \\ s_{61}^{\mathrm{p}} + fs_{61}^{\mathrm{m}} & s_{62}^{\mathrm{p}} + fs_{62}^{\mathrm{m}} & s_{66}^{\mathrm{p}} + fs_{66}^{\mathrm{m}} & d_{16} & d_{26} & d_{36} \\ d_{11} & d_{12} & d_{16} & \epsilon_{11} & \epsilon_{12} & \epsilon_{13} \\ d_{21} & d_{22} & d_{26} & \epsilon_{21} & \epsilon_{22} & \epsilon_{23} \\ d_{31} & d_{32} & d_{36} & \epsilon_{31} & \epsilon_{32} & \epsilon_{33} \end{bmatrix} \times \begin{bmatrix} \sigma_1^{\mathrm{p}} \\ \sigma_2^{\mathrm{p}} \\ \sigma_6^{\mathrm{p}} \\ E_1^{\mathrm{p}} \\ E_2^{\mathrm{p}} \\ E_3^{\mathrm{p}} \end{bmatrix} = \begin{bmatrix} q_{11}H_1 + q_{31}H_3 \\ q_{12}H_1 + q_{32}H_3 \\ q_{16}H_1 + q_{36}H_3 \\ 0 \\ 0 \\ 0 \end{bmatrix} \tag{18}$$

for the unknowns. We may again verify that the matrix is invertible and we can solve for the induced stresses and electric fields in terms of the applied magnetic field, and use them to compute the longitudinal and transverse magnetoelectric voltage coefficients as before. Again, these are too complicated to explore without numerics in the general case, but reduce to equations (16) and (17) in the case of an uniaxial piezoelectric that is normally oriented. In this situation of the insulating magnetic material, we also define an *in-plane longitudinal magnetoelectric voltage coefficient* $\alpha_{E,11} = E_1^{\mathrm{p}}/H_1$. While this is too complicated to explore without numerics in the general case, we obtain the following explicit expression in the case of

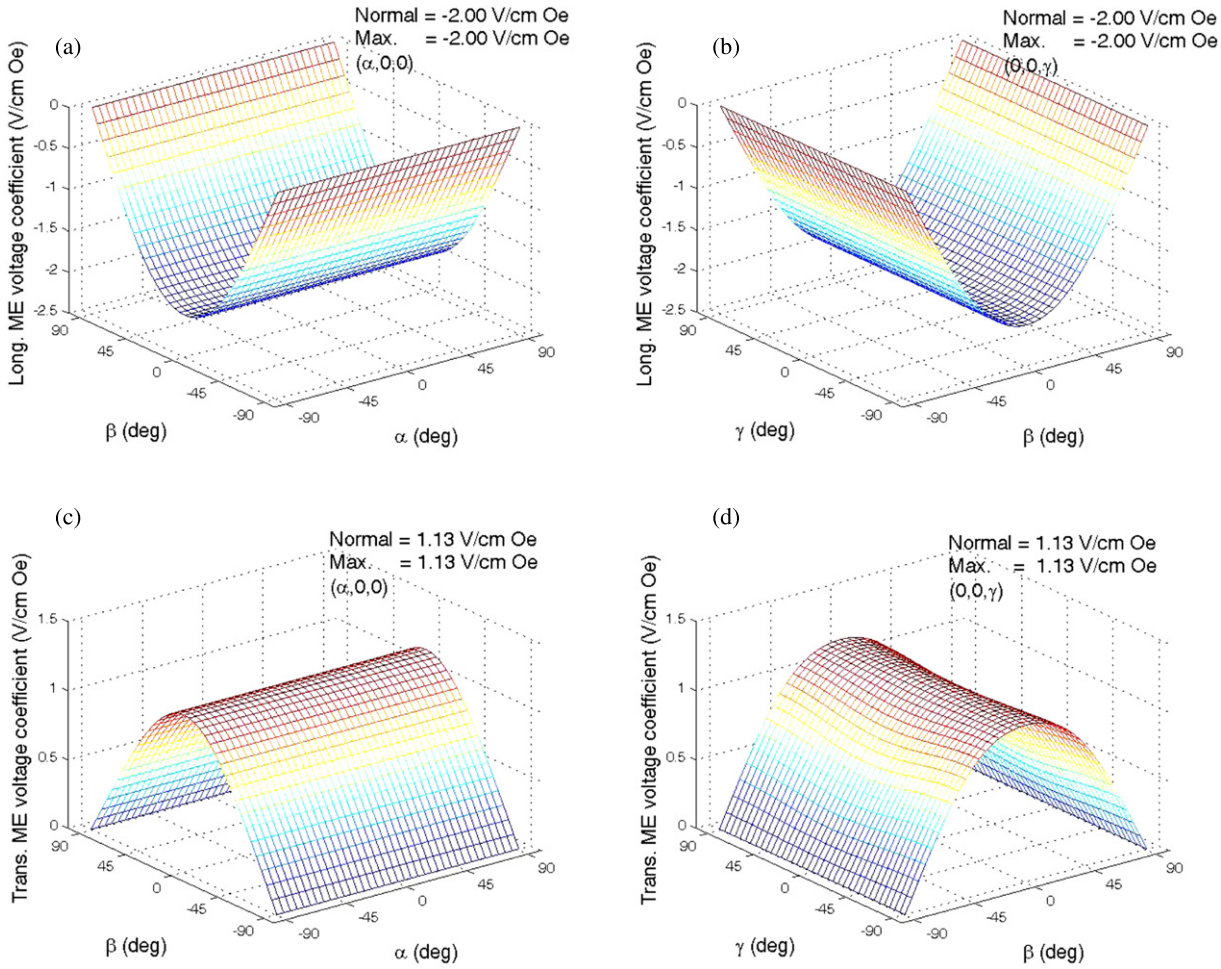

Figure 8. The ME voltage coefficient of a PZT/Terfenol-D bilayer for various orientations of PZT. (a), (b) The longitudinal coefficient for various PZT orientations. (c), (d) The transverse coefficient for various PZT orientations.

an uniaxial piezoelectric that is normally oriented:

$$\alpha_{E,11} = \frac{E_1^{\mathrm{p}}}{H_1} = [q_{11}(d_{11}s_{22}^{\mathrm{p}} - d_{12}s_{12}^{\mathrm{p}} + fd_{11}s_{22}^{\mathrm{m}} - fd_{12}s_{12}^{\mathrm{m}}) - q_{12}(d_{11}s_{12}^{\mathrm{p}} - d_{12}s_{11}^{\mathrm{p}} + fd_{11}s_{12}^{\mathrm{m}} - fd_{12}s_{11}^{\mathrm{m}})][\Delta]^{-1}, \quad (19)$$

where $\Delta = \epsilon_{11}[(s_{12}^{\mathrm{p}})^2 - s_{11}^{\mathrm{p}}s_{22}^{\mathrm{p}} - f(s_{11}^{\mathrm{m}}s_{22}^{\mathrm{p}} - 2s_{12}^{\mathrm{m}}s_{12}^{\mathrm{p}} + s_{11}^{\mathrm{p}}s_{22}^{\mathrm{m}}) + f^2((s_{12}^{\mathrm{m}})^2 - s_{11}^{\mathrm{m}}s_{22}^{\mathrm{m}})] + d_{12}^2 s_{11}^{\mathrm{p}} + d_{11}^2 s_{22}^{\mathrm{p}} - 2d_{11}d_{12}s_{12}^{\mathrm{p}} + f(d_{12}^2 s_{11}^{\mathrm{m}} + d_{11}^2 s_{22}^{\mathrm{m}} - 2d_{11}d_{12}s_{12}^{\mathrm{m}})$.

Finally, we come to the nonlinear setting of the piezoelectric/magnetostrictive material. Recall from equation (3) that the strain depends nonlinearly on the applied magnetic field. However, it turns out that we can follow exactly the same procedure as above and obtain equations (15) and (18) with the right-hand side replaced by

$$\begin{bmatrix} \lambda_1(H_i) \\ \lambda_2(H_i) \\ \lambda_6(H_i) \\ 0 \\ 0 \\ 0 \end{bmatrix}. \quad (20)$$

Thus, we can invert the matrix as before and obtain the induced electric field (as well as induced stress) as a function of the applied magnetic field. The induced electric field is a nonlinear function of the applied magnetic field, so we can either describe this as a magnetic-field-dependent magnetoelectric voltage coefficient or directly report the induced voltage as a function of the magnetic field. We choose to do the latter. Further, most magnetostrictive materials have a saturation strain and thus the induced electric field of the bilayer also has a saturation value. We focus on this value.

2.4. Optimization

We seek to optimize the magnetoelectric coefficient with respect to the crystallographic orientation of the materials. This is a highly nonlinear problem and there are a variety of approaches to solving this numerically [26]. However, all of these involve probing the local landscape and finding the local optimum. Unfortunately, this does not guarantee finding the global optimum that we seek. This is especially problematic in situations where one has multiple local optima and saddle points. This is, unfortunately, the situation in this problem, as we shall see in section 3. However, our problem has a low dimension and we resort to a brute-force approach where we create a fine grid of Euler angles and exhaustively compare the values on this grid.

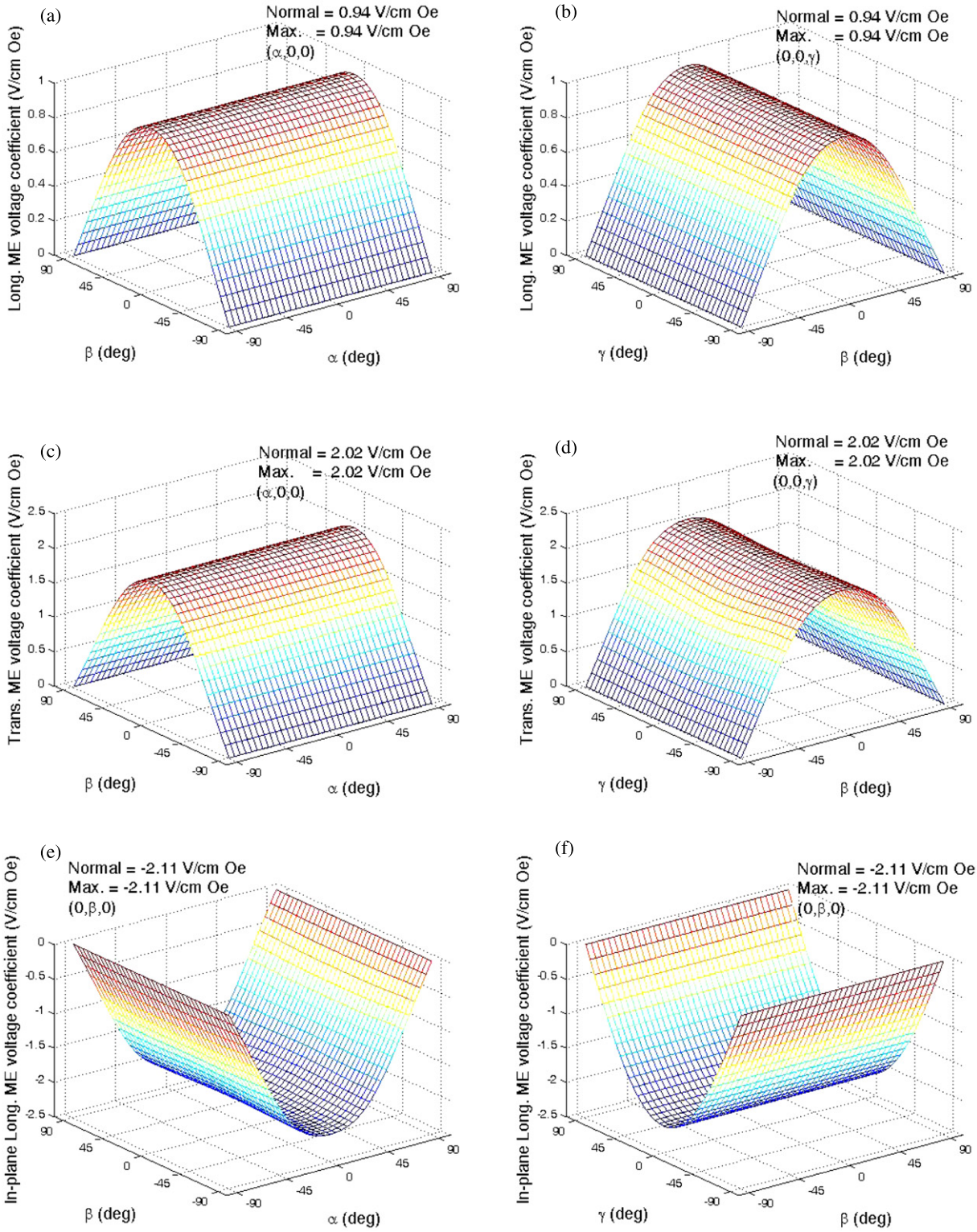

Figure 9. The ME voltage coefficient of a PZT/CFO bilayer for various orientations of PZT. (a), (b) The longitudinal coefficient for various PZT orientations. (c), (d) The transverse coefficient for various PZT orientations. (e), (f) The in-plane longitudinal coefficient for various PZT orientations.

3. Numerical results and optimization

We consider a variety of systems of interest. For the piezoelectric material, we consider the lead-free ferroelectric $LiNbO_3$ (3*m* symmetry) as well as the widely used poled PZT ceramic (6*mm* symmetry). For the piezomagnetic/magnetostrictive material we consider the giant magnetostrictive material Terfenol-D alloy (6*mm* symmetry) which is electrically conducting as

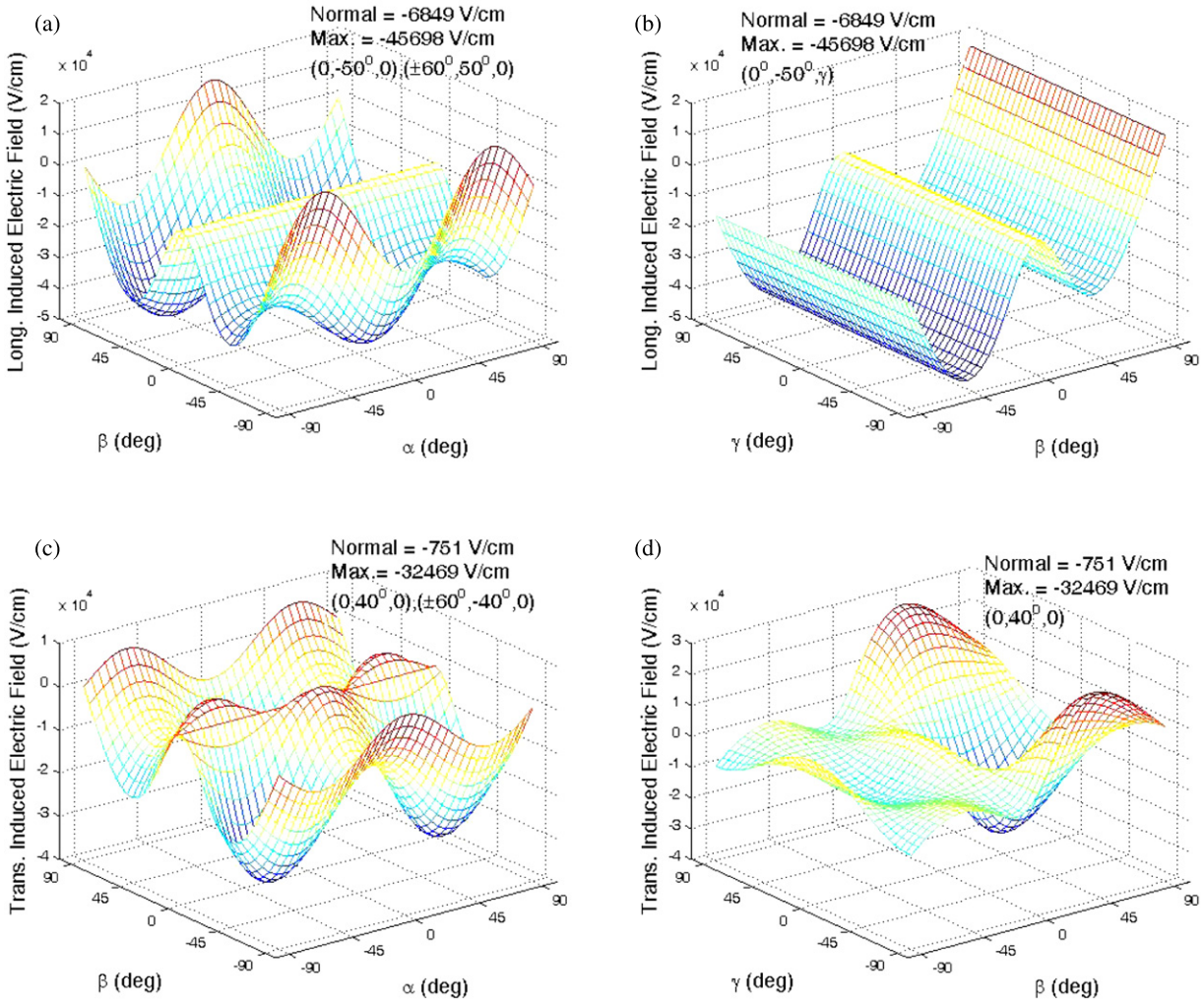

Figure 10. The magnetically induced electric field in a $LiNbO_3$/Terfenol-D bilayer due to the nonlinear magnetostrictive response of Terfenol-D. (a), (b) The longitudinal field for various $LiNbO_3$ orientations. (c), (d) The transverse field for various $LiNbO_3$ orientations.

well as the insulating $CoFe_2O_4$ (6*mm* symmetry). The material properties are listed in table 1 in Voigt notation. Some caution about factors of two and four is necessary to convert the Voigt notation to tensor notation. Also, there is uncertainty in the piezomagnetism of Terfenol-D and $CoFe_2O_4$ since it depends on the specific bias magnetic field.

3.1. Piezoelectric and piezomagnetic bilayers

We begin with the case of a piezoelectric and piezomagnetic bilayer. We first consider Terfenol-D as the magnetic layer and note that it is electrically conducting. For each orientation, we follow the procedure developed in section 2 to obtain the magnetoelectric voltage coefficients.

Figure 2 shows the longitudinal ME voltage coefficient $\alpha_{E,33}$ with respect to the crystallographic orientation of $LiNbO_3$. The orientation of Terfenol-D is the normal cut where the c axis coincides with the laminate normal x_3 since this happens be optimal and the volume fractions are equal. We observe that the maximum of -6.17 V cm^{-1} Oe^{-1} occurs at Euler angles $(\alpha, \beta, \gamma) = (\pm 60°, 50°, \gamma)$ or $(0°, -50°, \gamma)$, where γ is arbitrary. This degeneracy of optimal orientation reflects the 3*m* symmetry. Significantly, the optimized value of -6.17 V cm^{-1} Oe^{-1} is almost *seven* times higher than -0.92 V cm^{-1} Oe^{-1}, which is the value of the normal cut where the c axis of the $LiNbO_3$ is along the laminate normal.

We now turn to the transverse ME voltage coefficient $\alpha_{E,31}$ and its orientation dependence is shown in figure 3. The orientation of Terfenol-D is assumed to be parallel to the x_1 (optimal) and the volume fractions are equal. The maximum value is 8.72 V cm^{-1} Oe^{-1} at the optimal orientation $(\alpha, \beta, \gamma) = (0°, 40°, \pm 90°)$, and this is as much as *seventeen* times higher than the value of 0.51 V cm^{-1} Oe^{-1} at the normal cut. Further, it is almost *four* times the value of 2.31 V cm^{-1} Oe^{-1} obtained at the $[(zxtw) - 129°/30°]$ cut introduced by Yang *et al* [20].

Figure 4 shows the effect of volume ratio v^p/v^m on the ME coefficients. The maximum value is obtained at vanishing piezoelectric material. At a finite thickness ratio, the piezoelectric material resists the magnetically induced strain in the magnetostrictive material. This gives rise to internal stresses which reduce the strain and consequently ME strain. However, as the thickness of the piezoelectric material vanishes it is unable to resist the magnetically induced

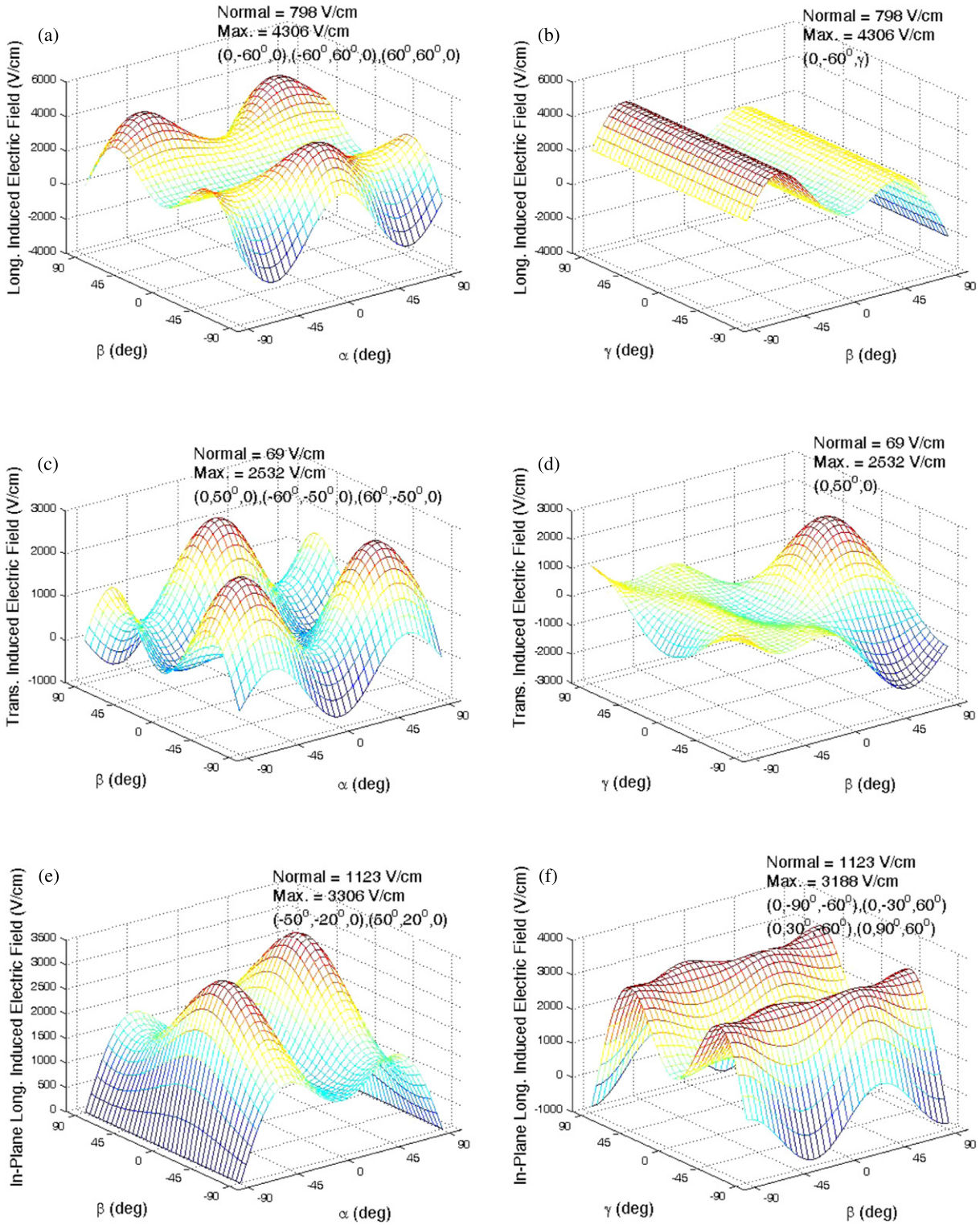

Figure 11. The magnetically induced electric field in a $LiNbO_3/CoFe_2O_4$ bilayer due to the nonlinear magnetostrictive response of CFO. (a), (b) The longitudinal field for various $LiNbO_3$ orientations. (c), (d) The transverse field for various $LiNbO_3$ orientations. (e), (f) The in-plane longitudinal field for various $LiNbO_3$ orientations.

strain, the internal stress vanishes and it suffers the full (stress-free) magnetically induced strain. The maximum value of the longitudinal coefficient $\alpha_{E,33}$ is -46.73 V cm^{-1} Oe^{-1} while that of the transverse coefficient $\alpha_{E,31}$ is 79.81 V cm^{-1} Oe^{-1}, both of these evaluated at their respective optimal orientations. Numerical calculations show that the optimal orientation is almost independent of the volume ratio.

To understand the role of electrical boundary conditions, we repeat these calculations with the $LiNbO_3/CoFe_2O_4$ bilayer since CFO is electrically insulating. We first consider

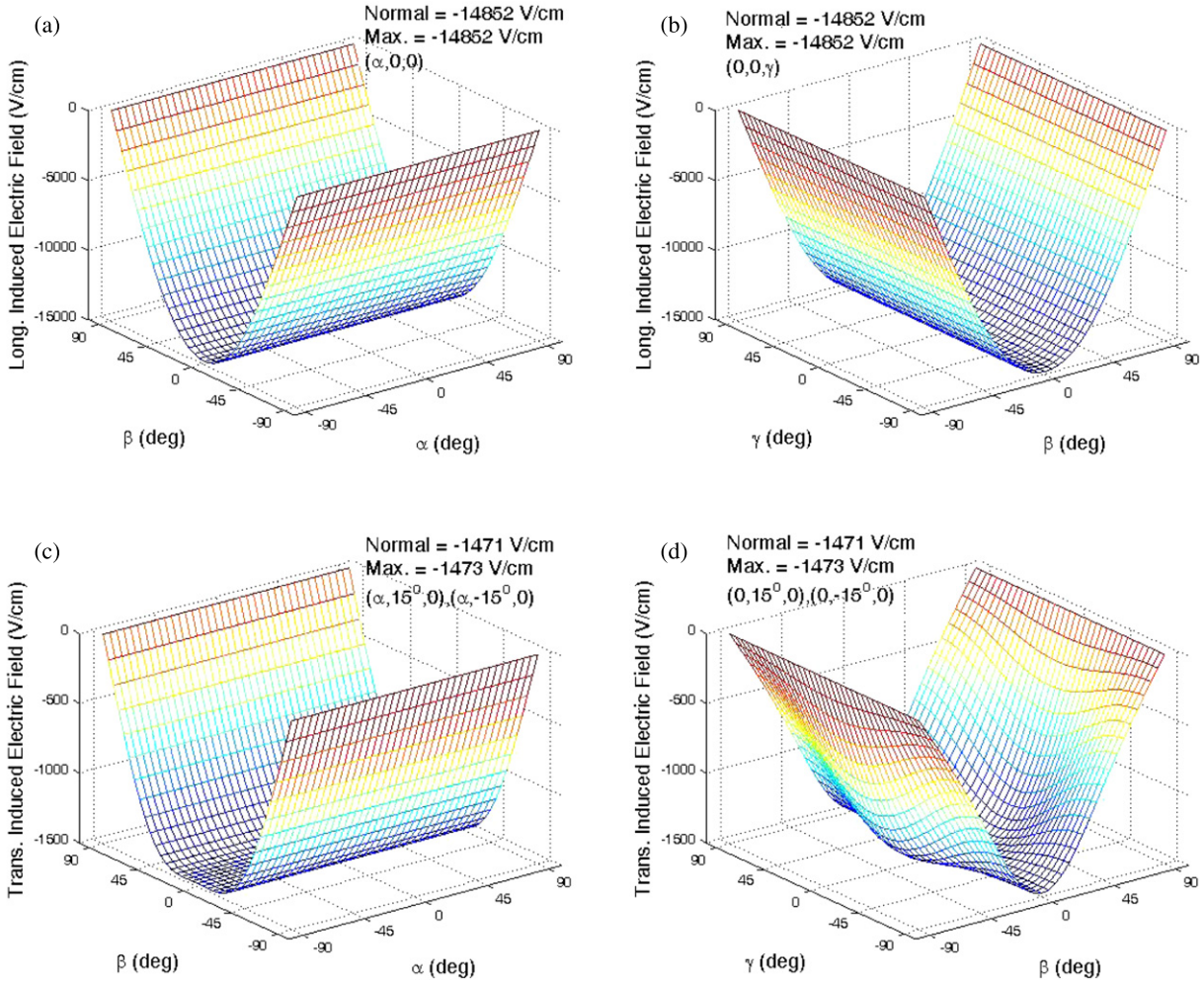

Figure 12. The magnetically induced electric field in a PZT/Terfenol-D bilayer due to the nonlinear magnetostrictive response of Terfenol-D. (a), (b) The longitudinal field for various PZT orientations. (c), (d) The transverse field for various PZT orientations.

the variation of the longitudinal magnetoelectric voltage coefficient $\alpha_{E,33}$ with respect to the orientation of the piezoelectric phase. The thickness of the two phases is the same. Figure 5 shows that the optimal is 2.77 V cm^{-1} Oe^{-1}, which is *five* times larger than that of the bilayer with the normal cut $LiNbO_3$ (0.51 V cm^{-1} Oe^{-1}). The corresponding optimal orientations are many and include Euler angles ($\pm 60°$, $60°$, γ) or ($0°$, $-60°$, γ) for arbitrary γ. In figure 6, we show the transverse magnetoelectric voltage coefficient $\alpha_{E,31}$ versus the orientation of the $LiNbO_3$ layer. It is optimized when $LiNbO_3$ is poled with $(\alpha, \beta, \gamma) = (0°, -60°, \pm 90°)$ with a value of 6.02 V cm^{-1} Oe^{-1}. Figure 7 shows the in-plane longitudinal magnetoelectric voltage coefficient $\alpha_{E,11}$ versus the orientation of the $LiNbO_3$ layer. It is optimized when $LiNbO_3$ is poled with $(\alpha, \beta, \gamma) = (-45°, 70°, 0°)$ or $(45°, -70°, 0°)$ and the coefficient is -6.78 V cm^{-1} Oe^{-1}. This is as much as *two* times the value of -3.52 V cm^{-1} Oe^{-1} at the normal cut.

We have also investigated the effect of volume ratio v^p/v^m on the longitudinal, transverse and in-plane longitudinal magnetoelectric voltage coefficients. The piezoelectric phase is poled along one of the optimized directions. The variations of the three cases are very similar to the conducting case, all increasing with the decreasing of the thickness of the piezoelectric phase. The maximum value of longitudinal coefficient $\alpha_{E,33}$ is 5.90 V cm^{-1} Oe^{-1} while that of the transverse coefficient $\alpha_{E,31}$ is 13.10 V cm^{-1} Oe^{-1}, and that of the in-plane longitudinal coefficient $\alpha_{E,11}$ is -15.15 V cm^{-1} Oe^{-1}. All of these are evaluated at their respective optimal orientation.

Finally, we replace the piezoelectric material by lead zirconate titanate (PZT) which is uniaxial (i.e. $6mm$). Now, the optimal orientation is the normal cut (i.e. c axis out of plane for $\alpha_{E,33}$ and $\alpha_{E,31}$ while in plane for $\alpha_{E,11}$) and the maximum $\alpha_{E,33}$ is -2.00 V cm^{-1} Oe^{-1} while the maximum $\alpha_{E,31}$ is 1.13 V cm^{-1} Oe^{-1} for the PZT/Terfenol-D bilayer at equal volume fraction (figure 8). Further, the maximum $\alpha_{E,33}$, $\alpha_{E,31}$ and $\alpha_{E,11}$ are 0.94, 2.02 and -2.11 V cm^{-1} Oe^{-1} for the PZT/$CoFe_2O_4$ bilayer at their normal orientation (figure 9).

3.2. Piezoelectric and magnetostrictive bilayers

We now turn to the nonlinear magnetostrictive response. We assume for simplicity that the saturation field is 2 kOe and

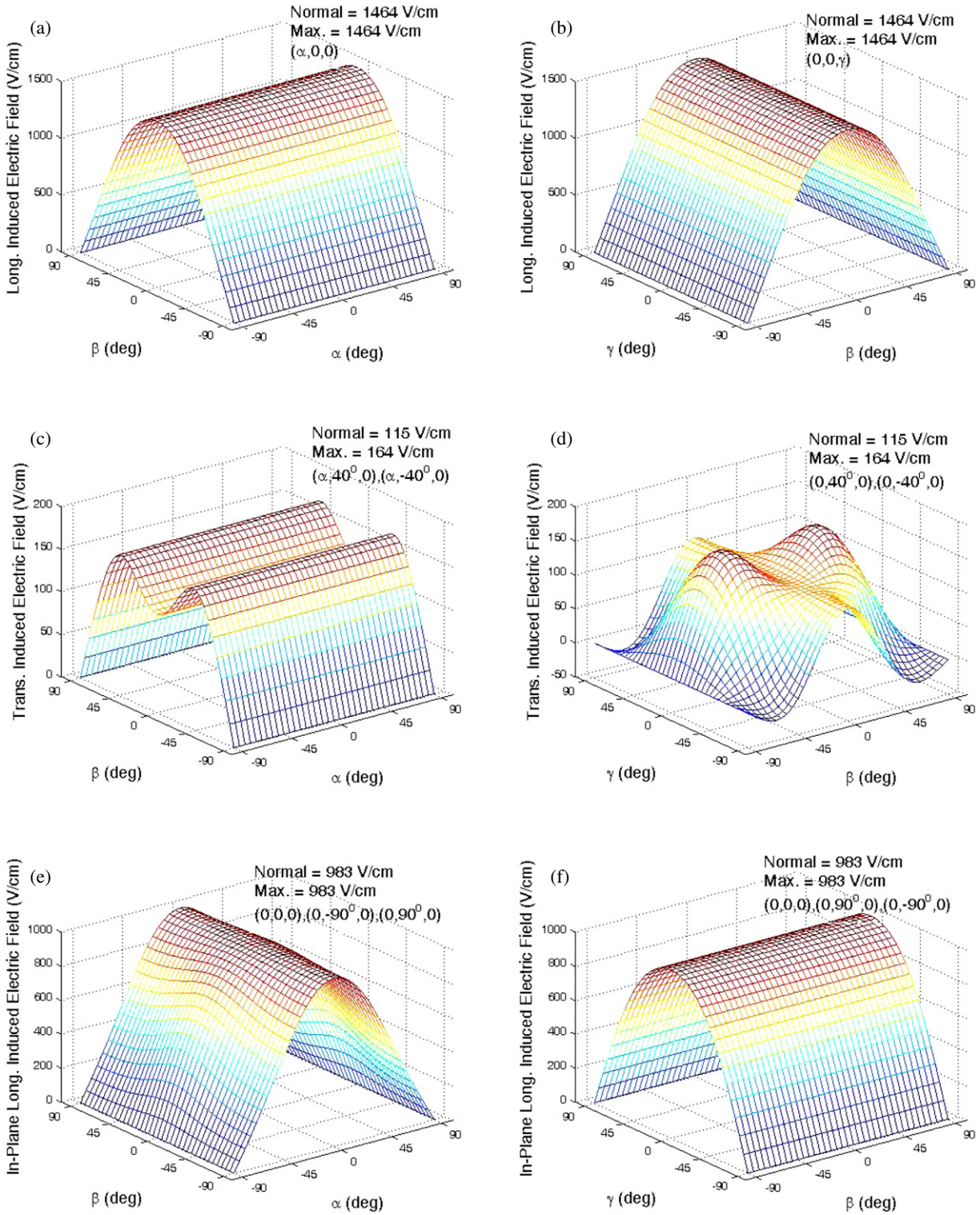

Figure 13. The magnetically induced electric field in a PZT/CFO bilayer due to the nonlinear magnetostrictive response of CFO. (a), (b) The longitudinal field for various PZT orientations. (c), (d) The transverse field for various PZT orientations. (e), (f) The in-plane longitudinal field for various PZT orientations.

study the induced electric field when this field is applied to the laminate. The longitudinal and transverse induced electric fields are shown in figure 10 as a function of orientation for the case where the volume fractions are equal. We find that the maximum induced electric field is -4.57×10^4 V cm^{-1} with $(\alpha, \beta, \gamma) = (0°, -50°, \gamma)$ or $(\pm 60°, 50°, 0°)$ for the longitudinal case and -3.25×10^4 V cm^{-1} with $(\alpha, \beta, \gamma) = (0°, 40°, 0°), (\pm 60°, -40°, 0°)$ for the transverse case. For the optimized volume fraction ($v^{\mathrm{p}} \rightarrow 0$), the numbers are -3.46×10^5 V cm^{-1} and -2.79×10^5 V cm^{-1}, respectively.

One may divide these number by 2 kOe to obtain the average ME coefficient; however, this is not a physical value since the response is highly nonlinear.

For the magnetically insulating case, the variation of the longitudinally, transversely and in-plane longitudinal induced electric field in the piezoelectric phase is shown in figure 11. The maximum longitudinal induced electric field is 4.31×10^3 V cm^{-1} with $(\alpha, \beta, \gamma) = (0°, -60°, \gamma)$ or $(\pm 60°, 60°, 0°)$ while the optimized transversely induced electric field is 2.53×10^3 V cm^{-1} with $(\alpha, \beta, \gamma) = (0°, 50°, 0°)$ or $(\pm 60°, -50°, 0°)$. The maximum in-plane longitudinal induced electric field is 3.30×10^3 V cm^{-1} with $(\alpha, \beta, \gamma) = (-50°, -20°, 0°)$ or $(50°, 20°, 0°)$. For the optimized volume fraction ($v^{\mathrm{p}} \to 0$), the numbers are 9.18×10^3 V cm^{-1}, 6.71×10^3 V cm^{-1} and 8.56×10^3 V cm^{-1}, respectively.

Finally, figures 12 and 13 show that, for the PZT and the nonlinear magnetostrictive laminate, the maximum longitudinal induced electric field is -14852 V cm^{-1} for the PZT/Terfenol-D bilayer and 1464 V cm^{-1} for the PZT/CFO case. Both of them are at their normal orientation. The maximum transverse induced electric field for the conducting case is -1473 V cm^{-1} at the optimal orientation $(\alpha, \beta, \gamma) = (\alpha, \pm 15°, 0°)$ and this is approximately the same as the value of -1471 V cm^{-1} at the normal cut. All of these increase significantly with thickness ratio in agreement with Dong *et al* [9]. For the insulating PZT/CFO, the maximum transverse induced electric field is 164 V cm^{-1} at $(\alpha, \beta, \gamma) = (\alpha, \pm 40°, 0°)$. This is approximately 40% higher than the value of 115 V cm^{-1} at the normal cut. The maximum in-plane longitudinal induced electric field is 983 V cm^{-1} at the normal cut.

4. Concluding remarks

In this work, we have proposed a simple framework to compute the effective magnetoelectric response of a piezoelectric–magnetostrictive bilayer. We have used it to show that, for anisotropic materials as in single crystals, the optimal ME response is obtained for non-trivial orientations. For the $LiNbO_3$/Terfenol-D bilayer, the highest transverse magnetoelectric voltage coefficient $\alpha_{E,31}$ at $v^{\mathrm{p}}/v^{\mathrm{m}} = 1$ is 8.72 V cm^{-1} Oe^{-1}, which is 17 times larger than that of a laminate made with the normal cut type $LiNbO_3$ single crystal. The longitudinal magnetoelectric voltage coefficient $\alpha_{E,33}$, on the other hand, can be increased around seven times to -6.17 V cm^{-1} Oe^{-1}. For the $LiNbO_3/CoFe_2O_4$ bilayer, the transverse and longitudinal magnetoelectric voltage coefficients can be increased around five times compared to the normal orientation. The in-plane longitudinal magnetolelectric voltage $\alpha_{E,11}$ can be increased around two times. The dependence of the magnetostrictive voltage coefficient with respect to the volume ratio $v^{\mathrm{p}}/v^{\mathrm{m}}$ was also determined when the lithium niobate was poled along the optimized direction. The coefficient varied with the volume ratio and was optimized when the thickness of the piezoelectric layer approaches zero.

In our model, we neglect flexure. A bilayer, especially of the structure shown on the left of figure 1, may have significant bending and this may also give rise to an additional ME effect especially when driven resonantly [32]. However, bending is a higher-order effect (bending strains scale as the third-power thickness while extensional strains considered here scale as thickness). Further, the coupling occurs through longitudinal strains similar to the situation studied here. So we anticipate that the optimal orientations will be close to those studied here. At the same time, since the strains are not uniform, the analysis becomes significantly more involved. This remains an issue for future work.

Acknowledgments

We gratefully acknowledge the financial support of the National Science Council, Taiwan (Taiwan Merit Scholarship to H-YK, 95-2211-E006-334-MY2), Caltech's SURF program (AS) and the US Army Research Office (AS and KB, W911NF-07-1-0410).

References

[1] Landau L D and Lifshitz E M 1984 *Electrodynamics of Continuous Media* (New York: Pergamon) p 119
[2] Astrov D N 1960 The magnetoelectric effect in antiferromagnetics *Sov. Phys.—JETP* **11** 708
[3] Rado G T and Folen V J 1961 Observation of the magnetically induced magnetoelectric effect and evidence for antiferromagnetic domains *Phys. Rev. Lett.* **7** 310
[4] Srinivasan G, Rasmussen E T, Levin B J and Hayes R 2002 Magnetoelectric effects in bilayers and multilayers of magnetostrictive and piezoelectric perovskite oxides *Phys. Rev.* B **65** 134402
[5] McGuire T R, Scott E J and Grannis F H 1956 Antiferromagnetism in a Cr_2O_3 crystal *Phys. Rev.* **102** 1000
[6] Eerenstein W, Mathur N D and Scott J F 2006 Multiferroic and magnetoelectric materials *Nature* **442** 759
[7] Nan C-W, Bichurin M I, Dong S, Viehland D and Srinivasan G 2008 Multiferroic magnetoelectric composites: historical perspective, status and future directions *J. Appl. Phys.* **103** 031101
[8] Ryu J, Carazo A V, Uchino K and Kim H-E 2001 Magnetoelectric properties in piezoelectric and magnetostrictive laminate composites *Japan. J. Appl. Phys.* **40** 4948
[9] Dong S, Zhai Z, Li J and Viehland D 2006 Near-ideal magnetoelectricity in high-permeability magnetostrictive/piezofiber laminates with a (2-1) connectivity *Appl. Phys. Lett.* **89** 252904
[10] Harshe G, Dougherty J O and Newnham R E 1993 Theoretical modelling of multilayer magnetoelectric composites *Int. J. Appl. Electromagn. Mater.* **4** 145
[11] Avellaneda M and Harshe G 1994 Magnetoelectric effect in piezoelectric magnetostrictive multilayer (2-2) composites *J. Intell. Mater. Syst. Struct.* **5** 501
[12] Nan C-W 1994 Magnetoelectric effect in composites of piezoelectric and piezomagnetic phases *Phys. Rev.* B **50** 6082
[13] Benveniste Y 1995 Magnetoelectric effect in composites with piezoelectric and piezomagnetic phases *Phys. Rev.* B **51** 16424
[14] Li J Y and Dunn M L 1998 Micromechanics of magnetoelectroelastic composite materials: average fields and effective behavior *J. Intell. Mater. Syst. Struct.* **9** 404

[15] Bichurin M I, Petrov V M and Srinivasan G 2002 Modeling of magnetoelectric effect in ferromagnetic/piezoelectric multilayer composites *Ferroelectrics* **280** 165
[16] Bichurin M I, Petrov V M and Srinivasan G 2002 Theory of low-frequency magnetoelectric effects in ferromagnetic–ferroelectric layered composites *J. Appl. Phys.* **92** 7681
[17] Bichurin M I, Petrov V M and Srinivasan G 2003 Theory of low-frequency magnetoelectric coupling in magnetostrictive–piezoelectric bilayers *Phys. Rev.* B **68** 054402
[18] Bichurin M I, Petrov V M, Averkin S V and Liverts E 2010 Present status of theoretical modeling the magnetoelectric effect in magnetostrictive–piezoelectric nanostructures. Part I: low frequency and electromechanical resonance ranges *J. Appl. Phys.* **107** 053904
[19] Park Y B, Diest K and Atwater H A 2007 Single crystalline $BaTiO_3$ thin films synthesized using ion implantation induced layer transfer *J. Appl. Phys.* **102** 074112
[20] Yang P, Zhao K, Yin Y, Wan J G and Shu J S 2006 Magnetoelectric effect in magnetostrictive/piezoelectric laminate composite Terfenol-D/$LiNbO_3$[(zxtw)129°/30°] *Appl. Phys. Lett.* **88** 172903
[21] Wang Y, Or S W, Chan H L W, Zhao X and Luo H 2008 Enhanced magnetoelectric effect in longitudinal–transverse mode Terfenol-D/$Pb(Mg_{1/3}Nb_{2/3})O_3$-$PbTiO_3$ laminate composites with optimal crystal cut *J. Appl. Phys.* **103** 124511
[22] Goldstein H 1980 *Classical Mechanics* (Reading, MA: Addison-Wesley)
[23] Gurtin M E 1981 *Introduction to Continuum Mechanics* (London: Academic)
[24] Tiersten H F 1990 *A Development of the Equations of Electromagnetism in Material Continua* (Berlin: Springer)
[25] Srinivasan G, Rasmussen E T, Gallegos J and Srinivasan R 2001 Magnetoelectric bilayer and multilayer structures of magnetostrictive and piezoelectric oxides *Phys. Rev.* B **64** 214408
[26] Ruszczynski A 2006 *Nonlinear Optimization* (Princeton, NJ: Princeton University Press)
[27] Xu Y 1991 *Ferroelectric Materials and Their Applications* (Amsterdam: North-Holland) p 226
[28] http://www.efunda.com/materials/piezo
[29] Liu Y X, Wan J G, Liu J-M and Wen C W 2003 Numerical modeling of magnetoelectric effect in a composite structure *J. Appl. Phys.* **94** 5111
[30] Teter J P, Wun-Fogle M, Clark A E and Mahoney K 1990 Anisotropic perpendicular axis magnetostriction in twinned $Tb_xDy_{1-x}Fe_{1.95}$ *J. Appl. Phys.* **67** 5004
[31] Bhame S D and Joy P A 2006 Tuning of the magnetostrictive properties of $CoFe_2O_4$ by Mn substitution for Co *J. Appl. Phys.* **100** 113911
[32] Chashin D V, Fetisov Y K, Tafintseva E V and Srinivasan G 2008 Magnetoelectric effects in layered samples of lead zirconium titanate and nickel films *Solid State Commun.* **148** 55